Available online at www.sciencedirect.com
ScienceDirect
Trans. Nonferrous Met. Soc. China 26(2016) 2960−2965
Transactions of Nonferrous Metals Society of China
www.tnmsc.cn

Catalytic reduction of SO_2 by CO over CeO_2−TiO_2 mixed oxides

Li ZHANG, Yi-hong QIN, Bai-zhen CHEN, Ya-guang PENG, Han-bing HE, Yi YUAN
School of Metallurgy and Environment, Central South University, Changsha 410083, China

Received 11 November 2015; accepted 18 May 2016

Abstract: The structure and catalytic desulfurization characteristics of CeO_2−TiO_2 mixed oxides were investigated by means of X-ray diffraction (XRD), X-ray photoelectron spectroscopy (XPS) and catalytic activity tests. According to the results, a CeO_2−TiO_2 solid solution is formed when the mole ratio of cerium to titanium n(Ce):n(Ti) is 5:5 or greater, and the most suitable n(Ce):n(Ti) is determined as 7:3, over which the conversion rate of SO_2 and the yield of sulfur at 500 °C reach 93% and 99%, respectively. According to the activity testing curve, $Ce_{0.7}Ti_{0.3}O_2$ (n(Ce):n(Ti)=7:3) without any pretreatment can be gradually activated by reagent gas after about 10 min, and reaches a steady activation status 60 min later. The XPS results of $Ce_{0.7}Ti_{0.3}O_2$ after different time of SO_2+CO reaction show that CeO_2 is the active component that offers the redox couple Ce^{4+}/Ce^{3+} and the labile oxygen vacancies, and TiO_2 only functions as a catalyst structure stabilizer during the catalytic reaction process. After 48 h of catalytic reaction at 500 °C, $Ce_{0.7}Ti_{0.3}O_2$ still maintains a stable structure without being vulcanized, demonstrating its good anti-sulfur poisoning performance.

Key words: CeO_2−TiO_2 mixed oxides; solid solution; catalytic reduction; carbon monoxide; sulfur dioxide

1 Introduction

Sulfur dioxide (SO_2), nitric oxide (NO) and carbon monoxide (CO) as by-products of combustion processes from industry, transportation and domestic activities are major components of atmospheric pollution. With the increasing environmental awareness, more and more researchers are committed to the development of efficient flue gas treatment technology. However, there is currently no widely accepted technology for the simultaneous treatment of NO, SO_2 and CO.

The catalytic reduction of SO_2 and NO to valuable sulfur and harmless N_2 by CO has been receiving much attention. ZHUANG et al [1,2] studied the reaction of NO−SO_2−CO on γ-alumina-supported sulfides of transition metals including CoMo and FeMo. They observed that stoichiometric catalytic reduction of NO and SO_2 to N_2 and elemental sulfur was achieved at 400 °C on the sulfided CoMo/Al_2O_3 and the sulfided FeMo/Al_2O_3. But both of them need sulfurization pretreatment before reaching the active phase. The resulting oxidized CoMo/Al_2O_3 regained its activity by in situ sulfurization with elemental sulfur produced by the reaction of SO_2 and carbonyl sulfide (COS). In contrast, the sulfided FeMo/Al_2O_3 was easily oxidized by NO but hardly re-sulfided under the test conditions. ZHANG et al [3] investigated the simultaneous catalytic reduction of SO_2 and NO by CO over TiO_2-promoted cobalt sulfides, and found that 71% NO conversion and 84% SO_2 conversion were achieved at 250 °C. The conversion rates of both NO and SO_2 were improved with the increase of temperature. However, much COS formed at higher temperature, resulting in a decrease of SO_2 selectivity to sulfur. ZHANG et al [4,5] had also studied the simultaneous catalytic reduction of SO_2 and NO by CO over titanium−tin solid solution catalysts. Experimental results showed that the conversion rates of SO_2 and NO at a temperature above 350 °C were greater than 91% and 99%, respectively. In the TiO_2−SnO_2 solid solutions, the stability of Sn was poorer than that of Ti, and Sn could be sulfided during the reaction process. HU et al [6] reviewed the efficient conversion of SO_2 and NO on rare earth mixed compounds at 600 °C, but the conversion of SO_2/NO decreases greatly with the decrease of reaction temperature.

As well known, cerium is the most abundant element in rare earth family [7], and cerium oxide (CeO_2) is one of the most reactive rare earth metal oxides [8]. Due to its ability to store/release oxygen as an oxygen

Corresponding author: Yi-hong QIN; Tel:+86-731-88830216 ; E-mail: qinyihong@163.com
DOI: 10.1016/S1003-6326(16)64426-6

reservoir via the redox shift between Ce^{4+} and Ce^{3+} under oxidizing and reducing conditions, CeO_2 has attracted much attention in the field of catalysis [9−11]. However, being poorly thermostable, pure CeO_2 will undergo rapid sintering at high temperatures, thus greatly decreasing its oxygen storage capacity. A common measure to overcome this problem is to introduce other metal ions into the ceria cubic structure, which can increase the temperature stability and oxygen storage capacity (OSC) of CeO_2.

In addition, CeO_2 can form solid solutions with ZrO_2, MnO_2, TiO_2, SiO_2 and PbO_2 [12]. Among them, TiO_2 has attracted strong attention due to its outstanding mechanical, thermal, electrical and photocatalytic properties [13−16]. The CeO_2−TiO_2 nanopowders have been used in not only the photocatalyst field [17−19], but also other catalytic applications [20−26].

However, there are few references about the application of CeO_2−TiO_2 mixed oxides in the simultaneous catalytic reduction of SO_2 and NO by CO. Compared with NO, SO_2 is usually more difficult to reduce, yet it is easy to cause the poisoning of catalyst. Therefore, the catalytic desulfurization activity of CeO_2−TiO_2 mixed oxides was studied.

2 Experimental

2.1 Preparation of catalyst

The catalyst was prepared via sol−gel method [27]. In a typical procedure, a certain amount of cerium nitrate ($Ce(NO_3)_2 \cdot 6H_2O$) solid was dissolved in 20 mL of anhydrous ethanol, then stoichiometric butyl titanate ($Ti(OC_4H_9)_4$) was dropped into alcohol solution under stirring to form a mixed solution with a total cation concentration of 0.02 mol/L. In the following process, acetic acid (CH_3COOH) was added to adjust the pH to 0.8 and 5 mL of deionized water was added to support a hydrolysis condition. After 30 min of reaction, the sol was aged at 40 °C to form gel. The obtained wet gel was dried at 105 °C for 12 h, and finally roasted in subsection at 600 °C for 4 h to obtain the TiO_2−CeO_2 mixed oxides catalyst.

2.2 Measurement of catalytic activity

A packed-bed reactor made of quartz (10 mm in inner diameter and 14 mm in outer diameter) was used for the activity test. 0.5 g of catalyst powder was put in the middle of the reactor. The reactor was laid in a tube experimental electrical furnace of which the temperature could be controlled automatically, and the temperature difference of the catalyst bed was controlled within the range of ±2 °C. The activity testing temperature was fixed at 500 °C, slightly higher than the boiling point of sulfur. After the catalyst was heated in air at 500 °C for 30 min, a gas mixture of 0.3% SO_2 and 0.6% CO (both in volume fraction, gas mixture supplied by Changsha Gao-Ke Gas Co. Ltd.), diluted with N_2, was fed to the reactor as reactants at a constant flow rate of 200 mL/min. The inlet and outlet gases were analyzed by an on-line flue gas analyzer (MRU VARIO-plus) and the conversion rate of SO_2 was calculated based on the intensity difference between the inlet SO_2 and outlet SO_2. The data for steady-state activity of the catalysts were collected after 2 h of testing.

2.3 Characterization of catalyst

The catalyst structure was determined by X-ray diffractometry using a Rigaku D/max 2000 XRD analyzer. Conditions of analysis were as follows: target Cu (0.15415 nm); scanning speed 10 (°)/min; scanning range (2θ) 10°−80°. In addition, the X-ray photoelectron spectra (XPS) were acquired on a VG ESCALAB5 electron spectrometer equipped with a Mg K_α radiation source ($h\nu$=123.6 eV). The main C 1s peak (Binding energy=284.6 eV), was chosen as an internal standard to calibrate the energy scale.

3 Results and discussion

3.1 XRD analysis of catalysts

Figure 1 shows the XRD patterns of CeO_2−TiO_2 oxide composites with different mole ratios of cerium to titanium. Pure TiO_2 and CeO_2 display the pure anatase phase structure (JCPDS 21−1272) and cubic fluorite phase structure (JCPDS 34−0394), respectively. All CeO_2−TiO_2 oxide composites with Ce to Ti mole ratio ≥5:5 exhibit the pure cubic fluorite phase structure, indicating the formation of CeO_2-like solid solutions. Their diffraction peaks become broader and weaker with the increase of TiO_2 content. The CeO_2−TiO_2 oxide composites (5:5>n(Ce):n(Ti)>1:9) are mixtures of anatase TiO_2 and cubic CeO_2. With the further decrease

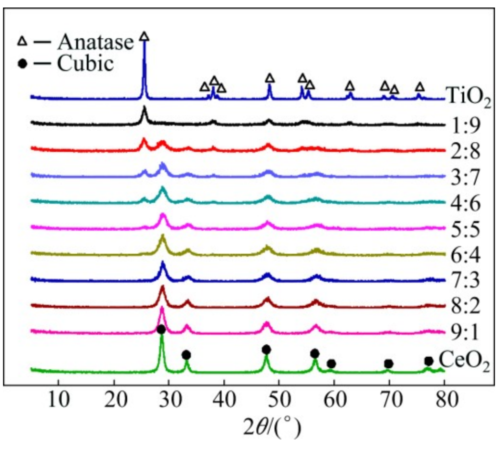

Fig. 1 XRD patterns of CeO_2−TiO_2 oxide composites with different Ce to Ti mole ratios

of Ce to Ti mole ratio (n(Ce)/n(Ti)≤1:9), the diffraction peaks of cubic CeO_2 disappear and the CeO_2-TiO_2 oxide composites are all pure anatase TiO_2, indicating the formation of TiO_2-like solid solutions. However, the diffraction peaks of a monoclinic phase mentioned in Ref. [28] have not been found, which may be attributed to the different preparation methods and procedures.

3.2 Activity of catalysts under different Ce to Ti mole ratios

CeO_2-TiO_2 mixed oxides with different Ce to Ti mole ratios were heated in air at 500 °C for 30 min. Then, a gas mixture of CO and SO_2 with a molar ratio of 2:1 (0.6% CO, 0.3% SO_2, in volume fraction) was fed into the reactor without any pretreatment. The weight-hourly- space velocity (WHSV) was fixed at 24000 mL/(h·g). The catalytic activation of CeO_2-TiO_2 mixed oxides with different Ce to Ti mole ratios in the CO+SO_2 reaction is shown in Fig. 2. The conversion rate of SO_2 over pure TiO_2 is only 48%, and the value increases with the increase of Ce to Ti mole ratios. When n(Ce):n(Ti) changes from 5:5 to 8:2, all of the conversion rates of SO_2 exceed 90 %, with the highest conversion rate of 93% when the n(Ce):n(Ti) ratio is equal to 7:3. After n(Ce):n(Ti) ratio reaches 9:1, the catalytic activity reduces obviously, and the catalytic activity of pure CeO_2 is about 80%, lower than that of n(Ce):n(Ti) ratio between 5:5 and 8:2. The high activity of catalyst when n(Ce):n(Ti) ratio is between 5:5 and 8:2 is mainly due to the formation of a solid solution. In the solid solution, Ce^{4+} and Ti^{4+} enter into the crystal lattice of each other, forming lattice distortion and thus resulting in various defect structures. These defect structures can not only enhance the adsorption capacity of surface (adsorb more SO_2), but also produce more oxygen vacancies (increase the oxygen storage capacity and the mobility of lattice oxygen). Under this condition, the catalytic activity of the mixed oxides is greatly improved. When the molar ratio of one ion to the other is too large (e.g. n(Ce):n(Ti)=9:1), some lattice defects may be associated in a certain way, leading to the healing of defects and the decrease of catalytic activity. Therefore, the most suitable molar ratio of Ti to Ce is determined as 7:3.

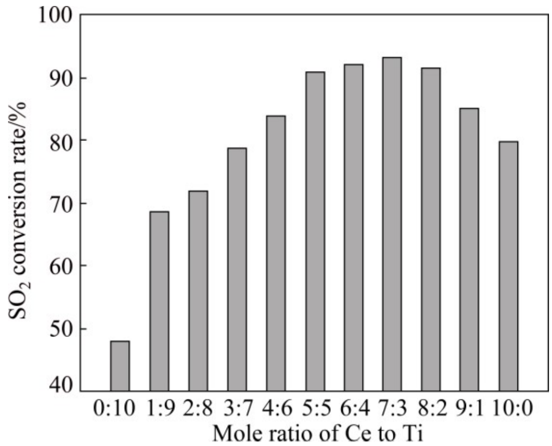

Fig. 2 Steady catalytic activity of CeO_2-TiO_2 mixed oxides with different Ce to Ti mole ratios in CO+SO_2 reaction

3.3 Characteristics of activity testing curve

The catalytic activity test of reducing SO_2 by CO over $Ce_{0.7}Ti_{0.3}O_2$ was carried out at 500 °C without any pretreatment and its catalytic desulfurization curve is shown in Fig. 3. It is found that the output of SO_2 in the effluent increases in the first 10 min, then decreases and stabilizes at the lowest platform after about 60 min. When the reactive gas mixture flows into the reactor, SO_2 may be greatly absorbed by the catalyst in the beginning (Fig. 3(a)). With the increase of the absorbed gas on the surface of the catalyst, the adsorption ability of the catalyst on SO_2 is reduced; hence, the output of SO_2 gradually increases. After about 10 min, the catalyst is activated, leading to the gradual decrease of the SO_2 output. Once the catalyst activation is completed (after about 60 min), the catalytic activity will reach a steady state, and the output of SO_2 will be stabilized at a platform.

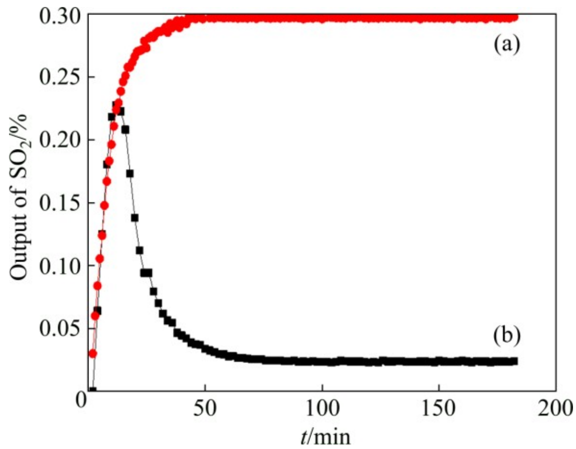

Fig. 3 Output of SO_2 in effluents over $Ce_{0.7}Ti_{0.3}O_2$ catalyst at 500 °C: (a) Adsorption curve of SO_2 (0.3% SO_2, catalyst mass 0.5 g, WHSV 24000 mL/(h·g)); (b) Reaction curve (0.3% SO_2 + 0.6% CO, catalyst mass 0.5 g, WHSV 24000 mL/(h·g))

Certain quantity of CO_2 is found in the gas outlet and elemental sulfur is also observed in the receiving flask after the reaction begins for a while. When the SO_2+CO reaction achieves its stability, the yield of sulfur, which is obtained by measuring the change of sulfur mass and the amount of removed SO_2 within a certain period of time, reaches about 99%.

3.4 Characteristics of catalytic reaction process

After different catalytic reaction time, the oxide catalysts were analyzed by XPS. The XPS spectra of

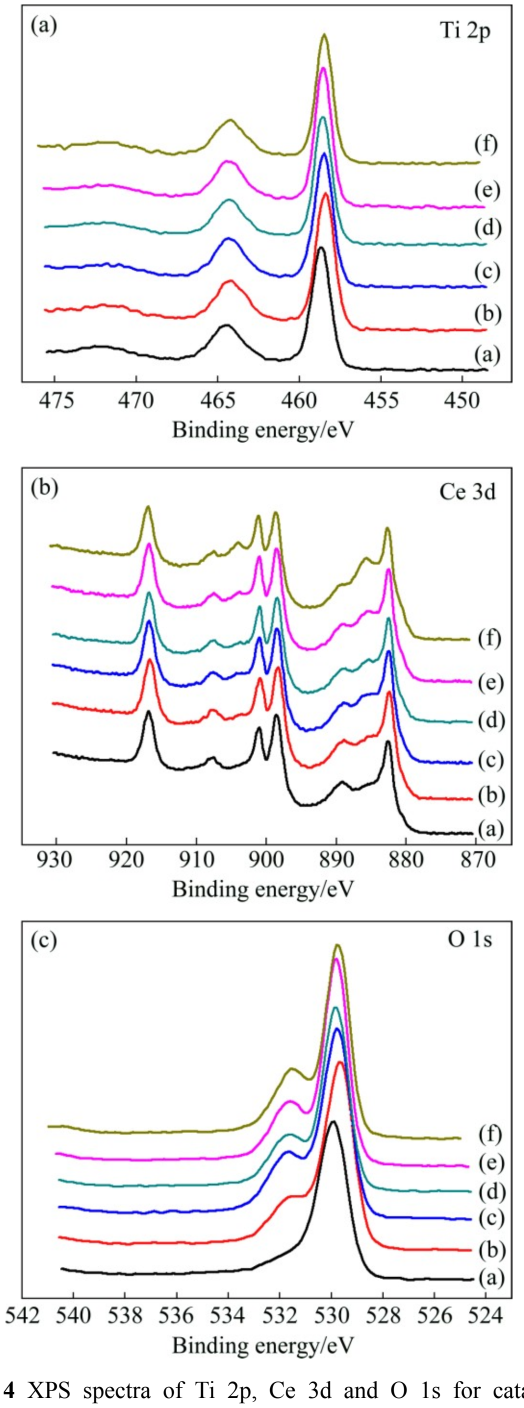

Fig. 4 XPS spectra of Ti 2p, Ce 3d and O 1s for catalyst $Ce_{0.7}Ti_{0.3}O_2$ with different reaction time: (a) 0 min; (b) 10 min; (c) 20 min; (d) 40 min; (e) 60 min; (f) 600 min

Ce 3d, Ti 2p and O 1s are shown in Fig. 4. Ti 2p spectra for the catalysts with different reaction time are similar to the fresh one, which only has peaks of Ti^{4+} at 464.4 eV (Ti $2p_{1/2}$) and 458.7 eV (Ti $2p_{3/2}$), without other states of titanium ions [29,30], illustrating that Ti^{4+} is not the redox species during the reaction process and is not the active substance. On the fresh catalyst, Ce 3d spectra have peaks at 916.5 eV (Ce $3d_{3/2}$) and 882.59 eV (Ce $3d_{5/2}$), which are the values of CeO_2. After about 10 min of reaction, the peaks at about 904 eV (Ce $3d_{3/2}$) and 885.6 eV (Ce $3d_{5/2}$) begin to appear in the Ce 3d XPS spectra. As the time of catalytic reaction increases, the two peaks are strengthened gradually. These changes in the Ce 3d XPS spectra indicate the increase of Ce^{3+} concentration on the surface of the catalyst [31,32]. In addition, the peaks of Ce^{4+} weaken with the increase of reaction time, suggesting that Ce^{4+} is reduced into Ce^{3+} gradually during the catalytic reaction and forms a high oxygen deficiency state. This assumption is also confirmed by O 1s spectra, which are broad and complicated because of the nonequivalence of surface oxygen ions. The Ce 3d XPS spectra can be also used to verify the variation of desulfurization curve.

3.5 Stability of catalyst

The phase compositions of $Ce_{0.7}Ti_{0.3}O_2$ powder before the catalytic reaction and after 48 h of catalytic reaction at 500 °C were analyzed by XRD, and the results are shown in Fig. 5.

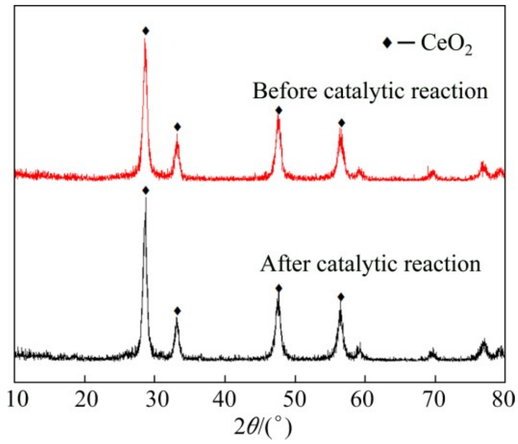

Fig. 5 XRD patterns before and after catalytic reaction

The structure of $Ce_{0.7}Ti_{0.3}O_2$ before and after the catalytic reaction does not change much, and only the main diffraction peak intensity of CeO_2 in cubic type has trace levels of enhancement after the catalytic reaction. This is possibly because that the $Ce_{0.7}Ti_{0.3}O_2$ crystal gets further perfect during the testing process at 500 °C. Thus, it can be seen that the catalyst $Ce_{0.7}Ti_{0.3}O_2$ maintains a stable structure without being vulcanized after 48 h of catalytic reaction.

The XPS survey spectra of the fresh and used (after de-SO_2) $Ce_{0.7}Ti_{0.3}O_2$ catalysts are shown in Fig. 6. There are mainly Ti, Ce and O on the surface of the catalyst, and C is the pollution source introduced by the test system. No obvious peak of S 2p is observed for the catalyst after desulfurization reaction. Both the XRD and XPS analysis results suggest that $Ce_{0.7}Ti_{0.3}O_2$ has good anti-sulfur properties.

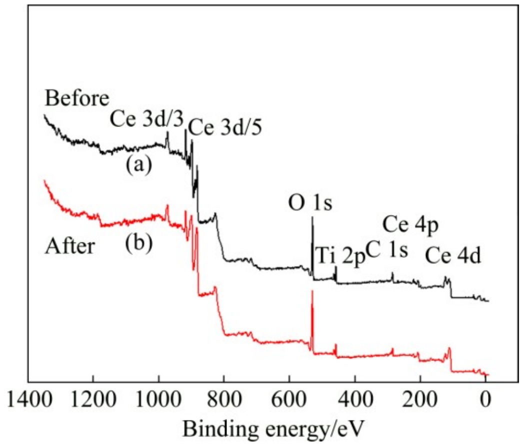

Fig. 6 XPS survey spectra of fresh (a) and used (b) $Ce_{0.7}Ti_{0.3}O_2$ catalysts

4 Conclusions

1) CeO_2-TiO_2 solid solution is formed when the mole ratio of cerium to titanium (n(Ce)/n(Ti)) is 5:5 or greater, and the most suitable n(Ce)/n(Ti) ratio is determined as 7:3, over which the SO_2 conversion rate and the stable yield of sulfur at 500 °C can reach 93% and 99%, respectively.

2) $Ce_{0.7}Ti_{0.3}O_2$ without any pretreatment may effectively absorb SO_2 at first, it is gradually activated after about 10 min, and reaches a steady activation status 60 min later. During the catalytic process, CeO_2 is the active component that offers the redox couple Ce^{4+}/Ce^{3+} and labile oxygen vacancies, and TiO_2 functions as a catalyst structure stabilizer.

3) Both the XRD and XPS results show that after 48 h of catalytic reaction at 500 °C, $Ce_{0.7}Ti_{0.3}O_2$ still maintains a stable structure without being vulcanized, demonstrating its good anti-sulfur poisoning performance.

References

[1] ZHUANG S X, MAGARA H, YAMAZAKI M, TAKAHASHI Y, YAMADA M. Catalytic conversion of CO, NO and SO_2 on the supported sulfide catalyst: I. Catalytic reduction of SO_2 by CO [J]. Applied Catalysis B: Environmental, 2000, 24(2): 89−96.

[2] ZHUANG S X, YAMAZAKI M, OMATA K, TAKAHASHI Y, YAMADA M. Catalytic conversion of CO, NO and SO_2 on the supported sulfide catalyst: II. Catalytic reduction of NO and SO_2 by CO [J]. Applied Catalysis B: Environmental, 2001, 31(2): 133−143.

[3] ZHANG Zhao-liang, MA Jun, YANG Xi-yao. Separate/simultaneous catalytic reduction of sulfur dioxide and/or nitric oxide by carbon monoxide over TiO_2-promoted cobalt sulfides [J]. Journal of Molecular Catalysis A: Chemical, 2003, 195(1−2): 189−200.

[4] ZHANG Zhao-liang, MA Jun, YANG Xi-yao. Separate/simultaneous catalytic reduction of sulfur dioxide and/or nitric oxide by carbon monoxide over titanium-tin solid solution catalysts [J]. Chemical Engineering Journal, 2003, 95(1): 15−24.

[5] ZHANG Zhao-liang, GENG Hao-ran, ZHENG Li-sheng, DU Bin. Resistance to sulfidation and catalytic performance of titanium-tin solid solutions in SO_2+CO and NO+SO_2+CO reactions [J]. Applied Catalysis A: General, 2005, 284(1−2): 231−237.

[6] HU Hui, WANG Shu-xia, ZHANG Xiao-ling, ZHAO Quan-zhong, LI Jin. Study on simultaneous catalytic reduction of sulfur dioxide and nitric oxide on rare earth mixed compounds [J]. Journal of Rare Earths, 2006, 24(6): 695−698.

[7] ZHU Yi, ZHANG Sheng-yi, SONG Ji-ming, MAO Chang-jie, NIU He-lin, JIN Bao-kang, TIAN Yu-peng. Synthesis and electrochemiluminescence of the CeO_2/TiO_2 composite [J]. Electrochimica Acta, 2011, 56(22): 7550−7554.

[8] FANG Jun, BI Xin-zhen, SI De-jun, JIANG Zhi-quan, HUANG Wei-xin. Spectroscopic studies of interfacial structures of CeO_2-TiO_2 mixed oxides [J]. Applied Surface Science, 2007, 253(22): 8952−8961.

[9] LOPEZ T, ROJAS F, ALEXZNDER-KATZ R, GALINDO F, BALANKIN A, BULJAN A. Porosity, structural and fractal study of sol−gel TiO_2-CeO_2 mixed oxides [J]. Journal of Solid State Chemistry, 2004, 177(6): 1873−1885.

[10] SANGEETHA P, CHEN Yu-wen. Preferential oxidation of CO in H_2 stream on Au/CeO_2-TiO_2 catalysts [J]. International Journal of Hydrogen Energy, 2009, 34(17): 7342−7347.

[11] LU Xiao-wang, QIAN Jun-chao, CHEN Feng, LI Xia-zhang, CHEN Zhi-gang. Synthesis, characterization and antibacterial property of Ag/mesoporous CeO_2 nanocomposite material [J]. Transactions of Nonferrous Metals Society of China, 2012, 22: 1418−1422.

[12] ZHU Zhi-hui, HE De-hua. CO hydrogenation to iso-C_4 hydrocarbons over CeO_2-TiO_2 catalysts [J]. Fuel, 2008, 87(10−11): 2229−2235.

[13] YANG Xi-jia, WANG Shu, SUN Hai-ming, WANG Xiao-bing, LIAN Jian-she. Preparation and photocatalytic performance of Cu-doped TiO_2 nanoparticles [J]. Transactions of Nonferrous Metals Society of China, 2015, 25: 504−509.

[14] CAO Guo-jian, CUI Bo, WANG Wen-qi, TANG Guang-ze, FENG Yi-cheng, WANG Li-ping. Fabrication and photodegradation properties of TiO_2 nanotubes on porous Ti by anodization [J]. Transactions of Nonferrous Metals Society of China, 2014, 24: 2581−2587.

[15] LUO Qiang, CAI Qi-zhou, LI Xin-wei, PAN Zhen-hua, LI Yu-jie, CHEN Xi-di, YAN Qing-song. Preparation and characterization of ZrO_2/TiO_2 composite photocatalytic film by micro-arc oxidation [J]. Transactions of Nonferrous Metals Society of China, 2013, 23: 2945−2950.

[16] TAO Jie, DENG Jie, DONG Xiang, ZHU Hong, TAO Hai-jun. Enhanced photocatalytic properties of hierarchical nanostructured TiO_2 spheres synthesized with titanium powders [J]. Transactions of Nonferrous Metals Society of China, 2012, 22: 2049−2056.

[17] HAO Chun-jing, LI Jing, ZHANG Zai-lei, JI Yong-jun, ZHAN Han-hui, XIAO Fang-xing, WANG Dan, LIU Bin, SU Fa-bing. Enhancement of photocatalytic properties of TiO_2 nanoparticles doped with CeO_2 and supported on SiO_2 for phenol degradation [J]. Applied Surface Science, 2015, 331: 17−26.

[18] AMEEN S, AKHTAR M S, SEO H K, SHIN H S. Solution-processed CeO_2/TiO_2 nanocomposite as potent visible light photocatalyst for the degradation of bromophenol dye [J]. Chemical Engineering Journal, 2014, 247: 193−198.

[19] MUNOZ-BATISTA M J, FERRER M, FERNANDEZ-GARCIA M, KUBACKA A. Abatement of organics and Escherichia coli using CeO_2-TiO_2 composite oxides: Ultraviolet and visible light performances [J]. Applied Catalysis B: Environmental, 2014, 154−155: 350−359.

[20] ZHANG Rui, ZHONG Qin, ZHAO Wei, YU Le-meng, QU Hong-xia. Promotional effect of fluorine on the selective catalytic reduction of

NO with NH_3 over CeO_2−TiO_2 catalyst at low temperature [J]. Applied Surface Science, 2014, 289: 237−244.
[21] ZHANG Lei, LI Lu-lu, CAO Yuan, YAO Xiao-jiang, GE Cheng-yan, GAO Fei, DENG Yu, TANG Chang-jin, DONG Lin. Getting insight into the influence of SO_2 on TiO_2/CeO_2 for the selective catalytic reduction of NO by NH_3 [J]. Applied Catalysis B: Environmental, 2015, 165: 589−598.
[22] CHAISUK C, WEHATORANAWEE A, PREAMPIYAWAT S, NETIPHAT S, SHOTIPRUK A, PANPRANOT J, JONGSOMJIT B, MEKASUWANDUMRONG O. Preparation and characterization of CeO_2/TiO_2 nanoparticles by flame spray pyrolysis [J]. Ceramics International, 2011, 37(5): 1459−1463.
[23] LI Hai-long, WU Chang-yu, LI Li-qing, LI Ying, ZHAO Yong-chun, ZHANG Jun-ying. Kinetic modeling of mercury oxidation by chlorine over CeO_2−TiO_2 catalysts [J]. Fuel, 2013, 113: 726−732.
[24] ZHAO Bin-xia, SHI Bin-chu, ZHANG Xiao-li, CAO Xin, ZHANG Yao-zhong. Catalytic wet hydrogen peroxide oxidation of H-acid in aqueous solution with TiO_2−CeO_2 and Fe/TiO_2−CeO_2 catalysts [J]. Desalination, 2011, 268(1−3): 55−59.
[25] LI Shu-na, ZHU Hua-qing, QIN Zhang-feng, WANG Guo-fu, ZHANG Ya-gang, WU Zhi-wei, LI Zhi-kai, CHEN Gang, DONG Wei-wen, WU Zhong-hua, ZHENG Li-rong, ZHANG Jing, HU Tian-dou, WANG Jian-guo. Morphologic effects of nano CeO_2−TiO_2 on the performance of Au/CeO_2−TiO_2 catalysts in low-temperature CO oxidation [J]. Applied Catalysis B: Environmental, 2014, 144: 498−506.
[26] CHEN Bu-ming, GUO Zhong-cheng, XU Rui-dong. Electrosynthesis and physicochemical properties of α-PbO_2−CeO_2−TiO_2 composite electrodes [J]. Transactions of Nonferrous Metals Society of China, 2013, 23: 1191−1198.
[27] CHEN Chun-liang, WENG Hung-shan. Nanosized CeO_2-supported metal oxide catalysts for catalytic reduction of SO_2 with CO as a reducing agent [J]. Applied Catalysis B: Environmental, 2005, 55: 115−122.
[28] LUO Meng-fei, CHEN Jun, CHEN Lin-shen, LU Ji-qing, FENG Zhao-chi, LI Can. Structure and redox properties of $Ce_xTi_{1-x}O_2$ solid solution [J]. Chemistry of Materials, 2000, 13(1): 197−202.
[29] DUTTA G, WAGHMARE U V, BAIDYA T, HEGDE M S, PRIOLKAR K R, SARODE P R. Origin of enhanced reducibility/oxygen storage capacity of $Ce_{1-x}Ti_xO_2$ compared to CeO_2 or TiO_2 [J]. Chemistry of Materials, 2006, 18(14): 3249−3256.
[30] FANG Jun, BAO Hui-zhi, HE Bo, WANG Fang, SI De-jun, JIANG Zhi-quan, PAN Zhi-yun, WEI Shi-qiang, HUANG Wei-xin. Interfacial and surface structures of CeO_2−TiO_2 mixed oxides [J]. The Journal of Physical Chemistry C, 2007, 111(51): 19078−19085.
[31] REDDY B M, KHAN A. Structural characterization of CeO_2−TiO_2 and V_2O_5/CeO_2−TiO_2 catalysts by Raman and XPS techniques [J]. The Journal of Physical Chemistry B, 2003, 107(22): 5162−5167.
[32] WATANABE S, MA Xiao-liang, SONG Chun-shan. Characterization of structural and surface properties of nanocrystalline TiO_2−CeO_2 mixed oxides by XRD, XPS, TPR, and TPD [J]. The Journal of Physical Chemistry C, 2009, 113(32): 14249−14257.

铈钛复合氧化物催化 CO 还原 SO_2

张 丽，秦毅红，陈白珍，彭亚光，何汉兵，袁 依

中南大学 冶金与环境学院，长沙 410083

摘 要：利用 X 射线衍射(XRD)，X 射线光电子能谱(XPS)及活性测试对铈钛复合氧化物的结构及催化脱硫特性进行了研究。结果表明：当铈−钛摩尔比(n(Ce)/n(Ti))≥5:5 时，铈钛复合氧化物形成固溶体；当 n(Ce)/n(Ti)=7:3(即 $Ce_{0.7}Ti_{0.3}O_2$)时，具有最佳的催化脱硫效果；500 °C 下 SO_2 的转化率达到 93%，单质硫的产率达到 99%。根据 $Ce_{0.7}Ti_{0.3}O_2$ 的活性测试曲线发现：未经预处理的 $Ce_{0.7}Ti_{0.3}O_2$ 约 10 min 后开始逐渐被反应气体活化，并在 60 min 后达到稳定活化状态。通过对不同反应时间下所得 $Ce_{0.7}Ti_{0.3}O_2$ 进行 XPS 分析发现： CeO_2 为活性物质，在反应过程中形成 Ce^{4+}/Ce^{3+}氧化还原电对和活性氧空位，而 TiO_2 仅起到稳定催化剂结构的作用。$Ce_{0.7}Ti_{0.3}O_2$ 催化 SO_2+CO 反应 48 h 后未出现硫化现象，始终保持结构的稳定，表现出较好的抗硫中毒性能。

关键词：铈钛复合氧化物；固溶体；催化还原；一氧化碳；二氧化硫

(Edited by Xiang-qun LI)